Electronic Supplementary Information

$2(C_3H_7N_6)^+ \cdot 2Cl^- \cdot H_2O$: An Ultraviolet Nonlinear Optical Crystal with Large Birefrigence and Strong Second-Harmonic Genertaion

Lehui Liu, [a] Chun-Li Hu,* [b] Zhiyong Bai, [a, c] Feifei Yuan, [a] Yisheng Huang, [a] Lizhen Zhang [a] and Zhoubin Lin* [a, d]

a. Key Laboratory of Optoelectronic Materials Chemistry and Physics, Fujian Institute of Research on the Structure of Matter, Chinese Academy of Sciences, Fuzhou 350002, P. R. China.

b. State Key Laboratory of Structural Chemistry, Fujian Institute of Research on the Structure of Matter, Chinese Academy of Sciences, Fuzhou, Fujian 350002, P. R. China.

c. University of the Chinese Academy of Sciences Beijing 100049, P. R. China.

d. Fujian Science & Technology Innovation Laboratory for Optoelectronic Information of China, Fuzhou, Fujian, 350108, P. R. China.

Experimental Procedures

Synthesis.

Experimental reagents. $H_6C_3N_6$ (98%, Aladdin), HCl (36%, Sinopharm). All chemicals above were used without further purification.

Synthesis of single crystal $2(C_3H_7N_6)^{+}\cdot 2Cl^{-}\cdot H_2O$ (HMELCl).

HMELCl was obtained by slow evaporation method in HCl-Water solution. First, $C_3H_6N_6$ (2 mmoL) was dissolved by 80 mL deionized water in a clean beaker with stirring and heating using magnetic stirrer at 40 ℃ until the solution became transparent. Then 1 mL HCl solution was added to the solution and stirred for one hour. After that the solution was let to a refrigerator and slowly evaporated at 277 K. After 10 days of growth, needle-shaped millimeter-sized crystals were grown. It was washed with deionized water, filtered with suction, and collected. The yield reached 73% (based on $C_3H_6N_6$).

Structure Determination.

The crystallographic data were collected on a Rigaku ROD, Synergy Custom bsystem, HyPix diffractometer equipped with a graphite monochromatic Ga Kα radiation (λ=1.3405Å). The CrysAlisPro and CrystalClear program were used for the data reduction, and absorption correction was run by the multi-scan method. In space group $Cmc2_1$, ShelXT was adopted to solve the structures and a ShelXL based on Olex2 was used to refine the structures [1]. By using PLATON, the structures of the title compounds were checked for possible symmetry absence, and none was discovered[2]. Information of Crystallographic data and structure refinements are given in Table S1; The atomic coordinates and equivalent isotropic displacement parameters are listed in Table S2; The anisotropic displacement parameters are listed in Table S3; The selected bond distances and angles are presented in Table S4-S5;The Torsion Angles are presented in Table S6.

Powder X-ray Diffraction.

Powder X-ray diffraction (PXRD) measurements were performed on a Rigaku MiniFlex 600 diffractometer equipped with a Cu Kα radiation (λ = 1.5406 Å) within the range of 2θ = 10-70° at 293K, with a step of 0.02° and an exposure of 1 s at each point. (Figure S1).

Energy Dispersive X-ray Spectroscope. Energy dispersive X-ray spectroscope (EDS, Oxford INCA) was used to microprobe elemental identification and analyses (Figure S2).

Thermal Stability.

Differential scanning calorimetry (DSC) and thermogravimetric analysis (TGA) were proceeded on a NETZSCH 449F3 instrument unit. About 10 mg of HMELCl were placed in Al_2O_3 crucible, heated at a rate of 5 K/min from 30°C to 800 °C under nitrogen system and then cooled to room temperature naturally (Figure S6).

Infrared Spectra Measurement.

The Infrared (IR) spectrum was performed on a VERTEX 70 FTIR spectrophotometer. The title compound was mixed thoroughly with dried KBr (~5 mg of the sample and 500 mg of KBr), and the IR spectrum was collected in the range from 400 to 4000 cm^{-1} with a resolution of 2 cm^{-1} (Figure S7).

UV−Vis−NIR Diffuse Reflectance Spectra Measurements.

UV-vis and NIR transmittance spectra measurements were implemented on a PerkinElmer Lambda 950 spectrophotometer within the range of 200-800 nm at room temperature (Figure S8).

Second-Harmonic Generation.

The polycrystalline SHG tests were measured by a modified Kurtz–Perry method using a Q-switched Nd: YAG solid-state laser under 1064 nm fundamental wave laser radiation. Polycrystalline samples of HMELCl and KDP (used as reference) were ground and sieved into the following particle sizes: 150-180, 110-150, 75-110, 55-75, 45-55, and 30-45 μm.

Birefringence Measurements.

The birefringence of HMELCl was characterized by using the polarizing microscope equipped (ZEISS Axio Scope. A1) with Berek compensator. The wavelength of the light source was 546 nm. Owing to the clear boundary lines of the first-, second- and third-order interference color, the relative error was small enough. Before the scanning, a small and transparent HMELCl lamellar crystal was chosen to measure, in order to improve the accuracy of the birefringence.

The formula for calculating the birefringence is listed below,

$R = | Ne - No | \times T = \Delta n \times T$ Eq. (1)

Here, R represents the optical path difference, Δn means the birefringence, and T denotes the thickness of the crystal.

Computational Descriptions.

Single-crystal structural data of HMELCl was used for the theoretical calculations. The electronic structures and optical properties were performed using plane-wave pseudopotentials method within density functional theory (DFT) implemented in the total energy code CASTEP [3]. For the exchange and correlation functional, we chose Perdew−Burke−Ernzerhof (PBE) in the generalized gradient approximation (GGA)[4]. The interactions between the ionic cores and the electrons were described by the norm-conserving pseudopotential[5]. The following valence-electron configurations were considered in the computation: H, $1s^1$;

C, $2s^22p^2$; N, $2s^22p^3$; O, $2s^22p^4$ and Cl $3s^23p^5$. The numbers of plane waves included in the basis sets were determined by a cut off energy of 750 eV. Monkhorst−Pack k-point sampling of $1 \times 2 \times 4$ was used to perform numerical integration of the Brillouin zone for HMELCl. Other parameters and convergent criteria were set as the default values of the CASTEP code. During the optical properties calculations, approximately 480 empty bands were involved to ensure the convergence of linear optical properties and SHG coefficients. The other parameters and convergent criteria were the default values of the CASTEP code. The calculations of second-order NLO properties were based on length-gauge formalism within the independent-particle approximation.[6] We adopted the Chen's formula in the static limit, which are given in Ref. 7.[7]

Results and Discussion

Table S1. Crystal data and structure refinement for HMELCl.

Identification code	$2(C_3H_7N_6)^+ \cdot 2Cl^- \cdot H_2O$
Empirical formula	$C_6H_{16}Cl_2N_{12}O$
Formula weight	343.21
Temperature/K	300.00(11)
Crystal system	orthorhombic
Space group	$Cmc2_1$
a/Å	16.7812(5)
b/Å	12.2467(4)
c/Å	6.9816(2)
α/°	90
β/°	90
γ/°	90
Volume/Å^3	1434.82(8)
Z	4
ρ_{calc}g/cm^3	1.589
μ/mm^{-1}	2.795
F(000)	712.0
Crystal size/mm^3	0.3 × 0.1 × 0.1
Radiation	GaKα (λ = 1.3405)
2Θ range for data collection/°	7.77 to 121.286
Index ranges	-20 ≤ h ≤ 21, -15 ≤ k ≤ 14, -8 ≤ l ≤ 8
Reflections collected	7725
Independent reflections	1523 [R_{int}= 0.0681, R_{sigma}= 0.0576]
Data/restraints/parameters	1523/1/124
Goodness-of-fit on F^2	1.025
Final R indexes [I>=2σ (I)]	R_1= 0.0394, wR_2= 0.0860
Final R indexes [all data]	R_1= 0.0501, wR_2= 0.0907
Largest diff. peak/hole / e Å^{-3}	0.27/-0.41
Flack parameter	0.05(3)

[a] $R_1 = \sum||F_o|-|F_c||/\sum|F_o|$ and $wR_2 = [\sum[w(F_o^2-F_c^2)^2]/\sum[w(F_o^2)^2]]^{1/2}$ for $F_0^2>2\sigma(F_c^2)$

Table S2. Fractional Atomic Coordinates (×10⁴) and Equivalent Isotropic Displacement Parameters (Å²×10³) for HMELCl. U_{eq} is defined as 1/3 of the trace of the orthogonalised U_{IJ} tensor.

Atom	*x*	*y*	*z*	U(eq)
Cl_1	5000	4286.5(10)	7523.3(17)	36.0(3)
Cl_2	5000	7818.5(9)	7650(2)	39.6(3)
N_1	3488.7(19)	3338(3)	5167(5)	37.3(7)
N_2	2327.8(15)	4196(2)	4297(4)	26.8(6)
N_3	1223.1(16)	5155(3)	3413(5)	32.8(6)
N_4	2302.7(15)	6162(2)	4310(4)	27.2(6)
N_5	3437.1(14)	5204(2)	5314(4)	27.2(6)
N_6	3431.5(19)	7071(3)	5272(5)	34.9(7)
C_1	1966.4(16)	5171(3)	4025(4)	23.6(6)
C_2	3072(2)	4229(3)	4917(5)	25.8(7)
C_3	3047(2)	6157(3)	4960(5)	26.0(7)
O_{1W}	5000	1570(3)	7353(9)	62.3(12)

Symmetry transformations used to generate equivalent atom:
'-x, -y, z+1/2' 'x, -y, z+1/2' '-x, y, z' 'x+1/2, y+1/2, z' '-x+1/2, -y+1/2, z+1/2' 'x+1/2, -y+1/2, z+1/2' '-x+1/2, y+1/2, z'

Table S3. Anisotropic Displacement Parameters (Å²×10³) for HMELCl. The anisotropic displacement factor exponent takes the form: $-2\pi^2[h^2a^{*2}U_{11}+2hka^*b^*U_{12}+\ldots]$.

Atom	U_{11}	U_{22}	U_{33}	U_{23}	U_{13}	U_{12}
Cl_1	20.7(5)	45.5(6)	41.8(5)	-0.7(7)	0	0
Cl_2	20.1(5)	37.8(6)	61.1(7)	-12.1(6)	0	0
N_1	20.7(15)	26.8(16)	64(2)	-5.2(17)	-6.4(14)	5.1(12)
N_2	19.0(12)	26.0(14)	35.4(14)	-1.9(12)	-1.7(10)	0.9(11)
N_3	19.8(13)	27.0(15)	51.6(16)	0.5(14)	-9.2(11)	0.1(12)
N_4	19.4(11)	24.7(14)	37.4(15)	0.7(12)	-3.2(10)	0.2(11)
N_5	14.3(11)	27.0(15)	40.2(15)	-2.8(14)	-5.4(10)	2.2(10)
N_6	22.3(15)	28.6(17)	53.8(18)	-1.2(16)	-7.8(12)	-2.6(12)
C_1	18.2(12)	24.7(16)	28.0(14)	-0.2(12)	-0.5(11)	1.2(11)
C_2	18.3(15)	27.3(17)	31.8(16)	0.1(14)	1.8(11)	2.1(13)
C_3	19.0(16)	28.1(18)	30.8(16)	-1.0(14)	0.3(12)	0.2(12)
O_{1W}	51(2)	42(2)	94(4)	3(3)	0	0

Table S4. Bond Lengths for HMELCl.

Atom	Atom	Length/Å	Atom	Atom	Length/Å
N_3	C_1	1.319(4)	N_2	C_2	1.322(4)
N_1	C_2	1.308(4)	N_5	C_3	1.361(4)
N_4	C_1	1.353(4)	N_5	C_2	1.371(4)
N_4	C_3	1.328(4)	N_6	C_3	1.311(4)
N_2	C_1	1.352(4)			

Table S5. Bond Angles for HMELCl.

Atom	Atom	Atom	Angle/°	Atom	Atom	Atom	Angle/°
C_3	N_4	C_1	116.0(3)	N_4	C_3	N_5	121.2(3)
C_2	N_2	C_1	116.3(3)	N_6	C_3	N_4	121.1(3)
C_3	N_5	C_2	119.7(3)	N_6	C_3	N_5	117.7(3)
N_3	C_1	N_4	117.1(3)	N_1	C_2	N_2	121.6(3)
N_3	C_1	N_2	117.2(3)	N_1	C_2	N_5	117.4(3)
N_2	C_1	N_4	125.7(3)	N_2	C_2	N_5	121.0(3)

Table S6. Torsion Angles for HMELCl.

A	B	C	D	Angle/°	A	B	C	D	Angle/°
C_1	N_4	C_3	N_5	-0.2(4)	C_3	N_5	C_2	N_1	175.8(3)
C_1	N_4	C_3	N_6	179.5(3)	C_3	N_5	C_2	N_2	-3.9(5)
C_1	N_2	C_2	N_1	-177.6(3)	C_2	N_2	C_1	N_3	-179.8(3)
C_1	N_2	C_2	N_5	2.1(4)	C_2	N_2	C_1	N_4	0.8(5)
C_3	N_4	C_1	N_3	178.8(3)	C_2	N_5	C_3	N_4	2.9(5)
C_3	N_4	C_1	N_2	-1.8(5)	C_2	N_5	C_3	N_6	-176.7(3)

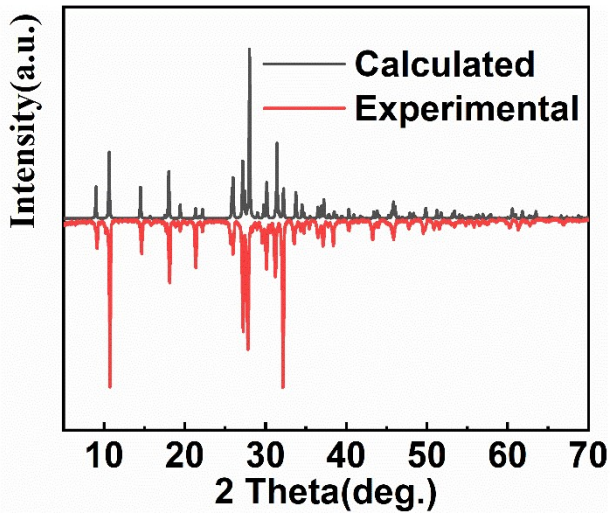

Figure S1. The experimental and simulated powder XRD patterns of HMELCl.

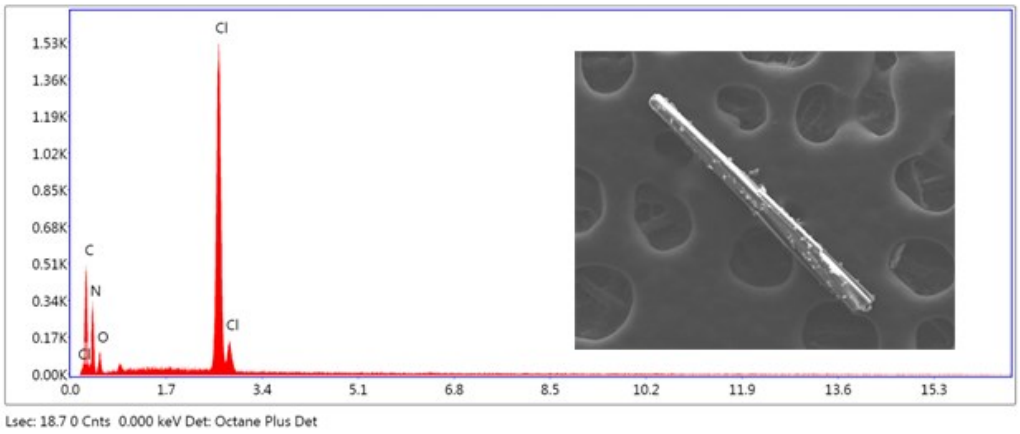

Figure S2. Energy dispersive X-ray spectroscopy (EDS) analysis of HMELCl.

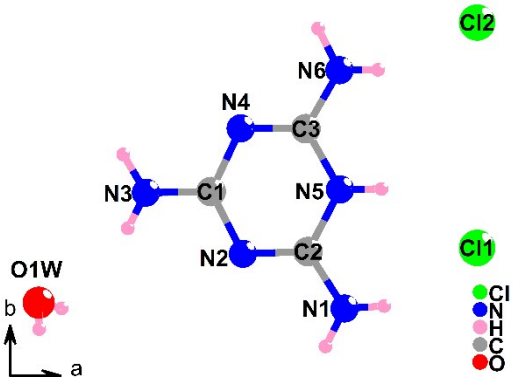

Figure S3. The asymmetric unit of HMELCl.

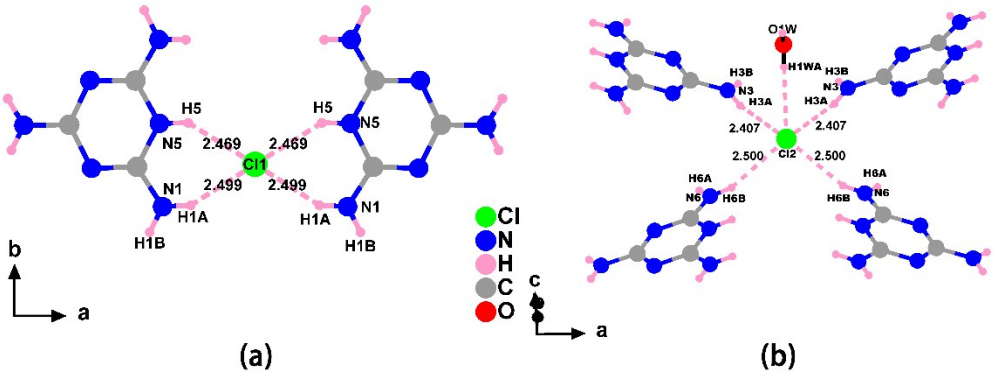

Figure S4. H-bonds of Cl1 and Cl2.

Table S7. Hydrogen-bonding geometry (Å, °).

Donor	H....Acceptor	D – H	H...A	D - H...A	D...H...A
N_1	Cl_1	0.81(5)	2.50(5)	3.239(3)	152(4)
N_5	Cl_1	0.86	2.47	3.244(3)	150
N_3	Cl_2	0.88(5)	2.40(4)	3.264(3)	168(3)
N_6	Cl_2	0.81(5)	2.49(5)	3.244(3)	157(3)
O_{1W}	Cl_2	0.85	2.75	3.368(6)	131
N_1	N_4	0.81(5)	2.23(5)	3.037(4)	178(7)
N_6	N_2	0.93(5)	2.05(5)	2.977(4)	179(6)

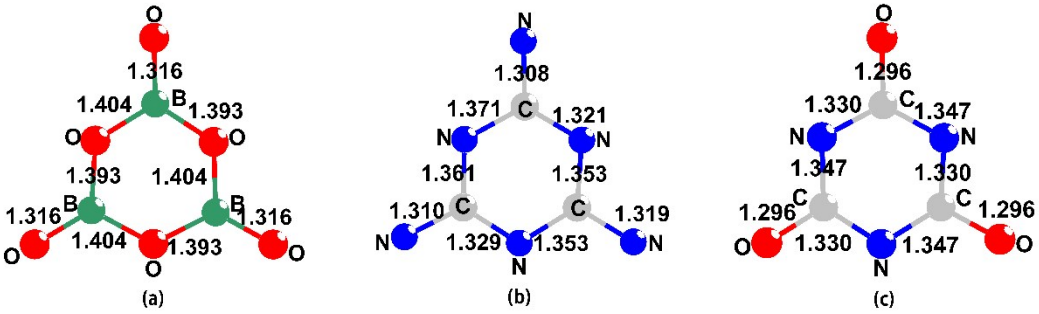

Figure S5. Comparison of β-BaB_2O_4 (a), HMELCl (b) and $Ca_3(O_3C_3N_3)_2$ (c).

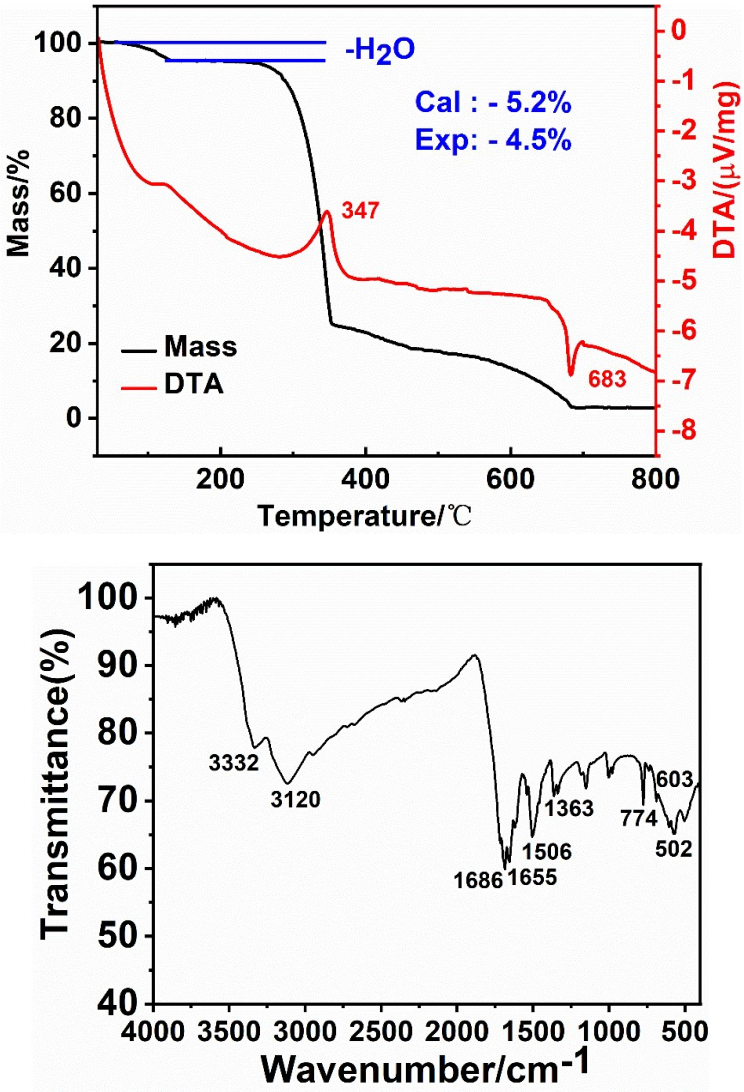

Figure S6. The TGA and DTA curves of HMELCl.

Figure S7. Room temperature powder IR spectrum of HMELCl.

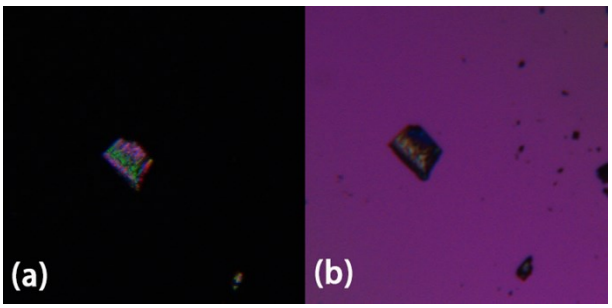

Figure S8. A comparison of (a) the original HMELCl crystal and (b) the HMELCl crystal achieving complete extinction.

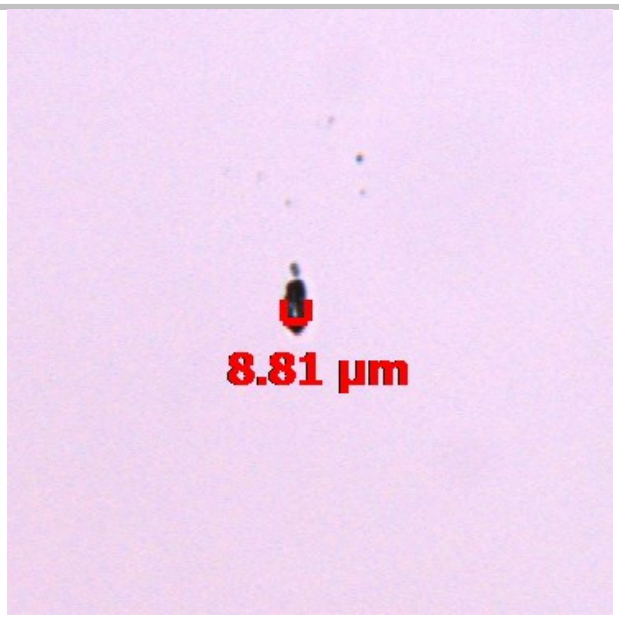

Figure S9 The thickness of HMELCl crystal.

Table S8. Optical properties of partially cyanurate to date

symmetry	no.	compound	abbreviation	Space group	SHG	Δ*n*	UV cutoff edges (nm)/Eg (eV)	ref
CS	1.	$K_2(HC_3N_3O_3)$	HCYK	*Cmcm*	null	0.35 at 800 nm	240/4.94	[8]
CS	2.	$LiRb(H_2C_3N_3O_3)_2{\cdot}2H_2O$	H_2CYLR	$P2_1/m$	null	>0.30	5.16	[9]
CS	3.	$LiCs(H_2C_3N_3O_3)_2{\cdot}2H_2O$	H_2CYLC	$P2_1/m$	null	>0.30	5.12	
CS	4.	$K_2Mg(H_2C_3N_3O_3)_4{\cdot}4H_2O$	H_2CYKM	*C*2/*m*	null	0.376 at 800 nm	230/5.38	[10]
CS	5.	$K_2Ca(H_2C_3N_3O_3)_4{\cdot}4H_2O$	H_2CYKC	*C*2/*m*	null	0.371 at 800 nm	233/5.32	
CS	6.	$Rb_2Ca(H_2C_3N_3O_3)_4{\cdot}4H_2O$	H_2CYRC	*C*2/*m*	null	0.362 at 800 nm	231/5.37	
CS	7.	$Cs_2Mg(H_2C_3N_3O_3)_4{\cdot}10H_2O$	H_2CYCM	$P\bar{1}$	null	N/A[a]	234/5.3	
NCS	8.	$NaCs_3(H_2C_3N_3O_3)_4{\cdot}3H_2O$	H_2CYNC	$Pmn2_1$	0.4 KDP	0.365 at 532 nm	227/5.46	[11]
NCS	9.	$Ca_3(C_3N_3O_3)_2$	CYC	*R3c*	d_{22} = 3.46 pm/V > 2 BBO	0.372 at 589.3 nm	N/A	[12]
NCS	10.	$Sr_3(C_3N_3O_3)_2$	CYS-β	*R3c*	d_{22} = 3.93 pm/V > 2 BBO	0.374 at 589.3 nm	N/A	
NCS	11.	$Eu_3(C_3N_3O_3)_2$	CYE	*R3c*	<BBO at 800 nm	N/A	N/A	[13]
NCS	12.	$Sr_3(C_3N_3O_3)_2$	CYS-*a*	*Cc*	>BBO at 800 nm	N/A	N/A	
NCS	13.	$K_6Cd_3(C_3N_3O_3)_4$	CYKC	$I\bar{4}3d$	d_{14} = 1.17 pm/V	null	237/5.23	[14]
CS	14.	$Ba_2Mg(C_3N_3O_3)_2$	CYBM	$R\bar{3}$	null	0.351 at 800 nm	230	[15]
CS	15.	$Ba_2Ca(C_3N_3O_3)_2$	CYBC	$R\bar{3}$	null	0.345 at 800 nm	225	
CS	16.	$Ba_2Sr(C_3N_3O_3)_2$	CYBS	$R\bar{3}$	null	0.35 at 800 nm	225/5.51	[16]
CS	17.	$Ba_2Pb(C_3N_3O_3)_2$	CYBP	$R\bar{3}$	null	0.31 at 800 nm	264/4.7	
CS	18.	$Li_2(HC_3N_3O_3){\cdot}2H_2O$	HCYL	$P2_1/c$	null	0.345 at 532 nm	5.05	[17]
CS	19.	$Rb_2(HC_3N_3O_3)$	HCYR	*Cmcm*	null	0.4 at 532 nm	4.96	
NCS	20.	$LiRb(HC_3N_3O_3){\cdot}2H_2O$	HCYLR	$Pna2_1$	2.7 KDP	0.259 at 532 nm	5.13	
NCS	21.	$NaRb_{0.86}Cs_{0.14}(HC_3N_3O_3){\cdot}2H_2O$	HCYNRC	$Pna2_1$	3 KDP	0.238 at 532 nm	5.16	
NCS	22.	$NaRb_3(H_2C_3N_3O_3)_4{\cdot}3H_2O$	H_2CYNR	$Pmn2_1$	0.67 KDP	0.389 at 532 nm	5.3	
NCS	23.	$LiK(HC_3N_3O_3){\cdot}2H_2O$	HCYKL	$Pna2_1$	3.1 KDP	0.280 at 532 nm	237/5.23	[18]
NCS	24.	$C_6N_{12}H_{14}^{2+}{\cdot}2Cl^{-}{\cdot}H_2O$	HMELCl	$Cmc2_1$	4.3 KDP/d_{31}=2.52 pm/V	0.277 at 546	245/4.7	This work

[a]N/A: not available

Reference

[1] a) G. M. Sheldrick, *Acta Crystallogr., Sect. A: Found. Crystallogr.* **2008**, *64*, 112-122; b) G. M. Sheldrick, *Acta Crystallogr., Sect. A: Found. Adv.* **2015**, *71*, 3-8; c) O. V. Dolomanov, L. J. Bourhis, R. J. Gildea, J. A. K. Howard, H. Puschmann, *J. Appl. Crystallogr.* **2009**, *42*, 339-341.

[2] A. L. Spek, *J. Appl. Crystallogr.* **2003**, *36*, 7-13.

[3] a) M. D. Segall, P. J. D. Lindan, M. J. Probert, C. J. Pickard, P. J. Hasnip, S. J. Clark, M. C. Payne, *J. Phys.: Condens. Matter* **2002**, *14*, 2717-2744; b) S. J. Clark, M. D. Segall, C. J. Pickard, P. J. Hasnip, M. J. Probert, K. Refson, M. C. Payne, *Zeitschrift Fur Kristallographie* **2005**, *220*, 567-570.

[4] J. P. Perdew, K. Burke, M. Ernzerhof, *Phys. Rev. Lett.* **1996**, *77*, 3865-3868.

[5] J. S. Lin, A. Qteish, M. C. Payne, V. V. Heine, *Phys. Rev. B: Condens. Matter Mater. Phys.* **1993**, *47*, 4174-4180.

[6] C. Aversa, J. E. Sipe, *Phys. Rev. B: Condens. Matter Mater. Phys.* **1995**, *52*, 14636-14645.

[7] J. Lin, M.-H. Lee, Z.-P. Liu, C. Chen, C. J. Pickard, *Phys. Rev. B: Condens. Matter Mater. Phys.* **1999**, *60*, 13380-13389.

[8] N. Wang, F. Liang, Y. Yang, S. Zhang, Z. Lin, *Dalton Trans.* **2019**, *48*, 2271-2274.

[9] X. Meng, F. Liang, J. Tang, K. Kang, T. Zeng, W. Yin, R. Guo, Z. Lin, M. Xia, *Inorg. Chem.* **2019**, *58*, 8948-8952.

[10] X. Meng, F. Liang, K. Kang, J. Tang, Q. Huang, W. Yin, Z. Lin, M. Xia, *Dalton Trans.* **2019**, *48*, 9048-9052.

[11] X. Meng, F. Liang, J. Tang, K. Kang, Q. Huang, W. Yin, Z. Lin, M. Xia, *Eur. J. Inorg. Chem.* **2019**, *2019*, 2791-2795.

[12] a) M. Kalmutzki, M. Strobele, F. Wackenhut, A. J. Meixner, H. J. Meyer, *Angew. Chem., Int. Ed.* **2014**, *53*, 14260-14263; b) M. Kalmutzki, M. Strobele, F. Wackenhut, A. J. Meixner, H. J. Meyer, *Inorg. Chem.* **2014**, *53*, 12540-12545.

[13] M. J. Kalmutzki, K. Dolabdjian, N. Wichtner, M. Strobele, C. Berthold, H. J. Meyer, *Inorg. Chem.* **2017**, *56*, 3357-3362.

[14] M. Xia, M. Zhou, F. Liang, X. Meng, J. Yao, Z. Lin, R. Li, *Inorg. Chem.* **2018**, *57*, 32-36.

[15] Z. Li, F. Liang, Y. Guo, Z. Lin, J. Yao, G. Zhang, W. Yin, Y. Wu, C. Chen, *J. Mater. Chem. C* **2018**, *6*, 12879-12887.

[16] K. Kang, F. Liang, X. Meng, J. Tang, T. Zeng, W. Yin, M. Xia, Z. Lin, B. Kang, *Inorg. Chem.* **2019**, *58*, 9553-9556.

[17] J. Lu, Y. K. Lian, L. Xiong, Q. R. Wu, M. Zhao, K. X. Shi, L. Chen, L. M. Wu, *J. Am. Chem. Soc.* **2019**, *141*, 16151-16159.

[18] D. Lin, M. Luo, C. Lin, F. Xu, N. Ye, *J. Am. Chem. Soc.* **2019**, *141*, 3390-3394.